1,4,5,6-Tetrahydropyrrolo[3,4-*c*]pyrazoles: Identification of a Potent Aurora Kinase Inhibitor with a Favorable Antitumor Kinase Inhibition Profile

Daniele Fancelli,[†] Jürgen Moll, Mario Varasi,[‡] Rodrigo Bravo, Roberta Artico,[§] Daniela Berta, Simona Bindi, Alexander Cameron, Ilaria Candiani, Paolo Cappella, Patrizia Carpinelli, Walter Croci, Barbara Forte, Maria Laura Giorgini, Jan Klapwijk,[||] Aurelio Marsiglio, Enrico Pesenti, Maurizio Rocchetti, Fulvia Roletto, Dino Severino, Chiara Soncini,[⊥] Paola Storici, Roberto Tonani, Paola Zugnoni, and Paola Vianello*

Nerviano Medical Sciences S.r.l. viale Pasteur 10, 20014 Nerviano, Milan, Italy

Received July 28, 2006

The optimization of a series of 5-phenylacetyl 1,4,5,6-tetrahydropyrrolo[3,4-*c*]pyrazole derivatives toward the inhibition of Aurora kinases led to the identification of compound **9d**. This is a potent inhibitor of Aurora kinases that also shows low nanomolar potency against additional anticancer kinase targets. Based on its high antiproliferative activity on different cancer cell lines, favorable chemico-physical and pharmacokinetic properties, and high efficacy in in vivo tumor models, compound **9d** was ultimately selected for further development.

Introduction

Mammalian Aurora kinases constitute a small family of three closely related Ser/Thr protein kinases, namely, Aurora-A, -B, and -C. They have different functions, subcellular localization, or timing of expression and are essential to secure the correct progress of cell cycle during mitosis or meiosis.[1,2] In fact, they are key regulators of major mitotic events such as centrosome maturation and separation, mitotic spindle assembly, chromosome separation, and cytokinesis.[2] Several lines of evidence indicate Aurora-A and -B as attractive targets for pharmacological intervention in oncology because, for example, both are found to be overexpressed in cancer.[3,4] The gene locus of Aurora-A maps to 20q13, a chromosomal region frequently amplified in a variety of human tumors.[5] Aurora-A can act as an oncogene because overexpression of Aurora-A leads to cell transformation in vitro,[6] and transgenic mice overexpressing Aurora-A in the mammary gland develop mammary tumors at a high incidence.[7] Finally, "small molecule" inhibitors of Aurora kinases demonstrate efficacy in animal tumor models, and the first compounds have entered clinical studies.[8−10]

We have previously described a novel series of Aurora kinases inhibitors identified from the combinatorial expansion of the 1,4,5,6-tetrahydropyrrolo[3,4-*c*]pyrazole bi-cycle, a versatile scaffold designed to target the ATP pocket of protein kinases.[11] In particular, the development of the pyrrolopyrazole subclasses characterized by a urea substituent at position 5 led to the identification of PHA-680632 (**1**), which demonstrated high in vitro antiproliferative activity on a wide range of cancer cell lines and significant tumor growth inhibition in different animal tumor models at well-tolerated doses.[12]

In this paper, we describe the optimization of the analogue 5-amido-pyrrolopyrazole subclasses, up to the identification and preliminary characterization of a potent Aurora inhibitor selected for evaluation as a potential anticancer agent.

* To whom correspondence should be addressed. Phone: +39.0331.581333. Fax: +39.0331.581347. E-mail: paola.vianello@nervianoms.com.
[†] Present address: Congenia, Italy.
[‡] Present address: DAC, Italy.
[§] Present address: Italfarmaco, Italy.
[||] Present address: GlaxoSmithKline, U.K.
[⊥] Present address: Università degli Studi di Milano, Italy.

Several 5-amido derivatives endowed with good Aurora-A inhibitory activity were initially identified through a preliminary combinatorial expansion of the pyrrolopyrazole scaffold. All these early hits were characterized by an arylacetic substituent at position 5 such as compounds **2** and **3** (Table 1).[11]

To highlight areas for possible optimization of the inhibitory activity, the crystal structure of compound **3** was solved as a complex with Aurora-A kinase and refined at a resolution of 2.0 Å (Figure 1).

As would be expected, the binding mode of **3** is very similar to that reported for PHA-680632 (**1**). However, the 5-amido-thiophene substituent adopts a different spatial position to the urea-containing compound. Rather than being situated under the glycine-rich loop, as is the case for the diethyl-phenyl urea group of PHA-680632, the amido-thiophene is directed away from the loop and packs around Leu 263. It was envisaged, therefore, that a substituent at the pro-R position of the benzylic methylene could adopt a position similar to the diethyl benzene of PHA-680632 under the glycine-rich loop and near to the amino nitrogen of Lys 162. In the structure reported here, such a substituent would be blocked by the presence of the activation loop that adopts a position with His 280 packing onto the aryl ring of the inhibitor. However, because this loop is very flexible and in other Aurora-A structures is not seen, its position in this structure was not thought to be of importance with regard to what substituents would fit in the binding site. Substitutions at the pro-S position were thought to be less favorable due to the proximity of Val 147.

Following this hypothesis and assuming that the phenyl group of compound 2 would adopt the same position as the thiophene of compound 3, we undertook the synthesis of a small series of pyrrolopyrazoles branched to the CH_2 of the phenylacetyl moiety in position 5, mainly with H-bond acceptor groups targeting a possible interaction with the Lys 162 hydrogens. In this series, we kept fixed at position 3 the already optimized 4-(1-methyl-piperazin-4-yl)benzamide, which in the analogue 5-urea subclasses provided inhibitors endowed with adequate aqueous solubility and high potency in cellular assays.

The general synthetic route outlined in Scheme 1 was used to prepare the target compounds **9a**−**f**.

The synthesis of the common intermediate **7** from the 5-Boc-protected 3-amino-tetrahydropyrrolo[3,4-*c*]pyrazole scaffold (**4**)

10.1021/jm060897w CCC: $33.50
Published on Web 11/01/2006

Table 1. Structure and Aurora-A Inhibition of PHA-680632 and Initial 5-Amido-pyrrolopyrazoles

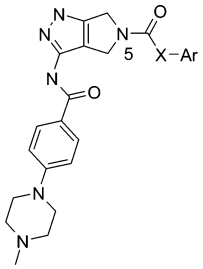

compd	X	Ar	Aur-A, IC_{50},[a] nM
1	NH	2,6-diethylphenyl	27
2	CH_2	phenyl	140
3	CH_2	2-thienyl	65

[a] IC_{50} values are reported as the mean of at least three individual determinations. Variability around the mean was <25%.

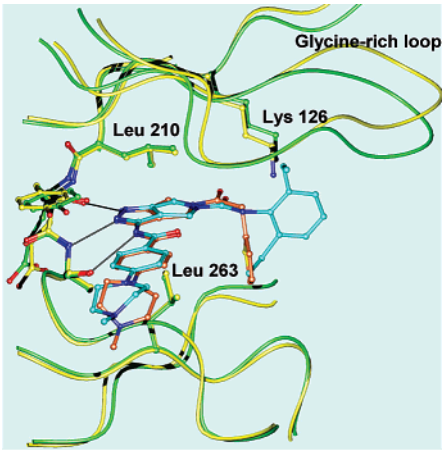

Figure 1. Structure of Aurora-A in complex with compound **3** (yellow, tan carbon atoms) superposed on the structure with PHA-680632 (**1**; light blue carbon atoms).

was performed as described in our previous report through protection of the pyrazole moiety with ethyl carbamate, *N*-acylation with *p*-piperazinylbenzoic acyl chloride, and Boc removal with HCl in dioxane.[11] The available pyrrolidinic nitrogen of **7** easily reacted with activated acids to give compounds **8a**−**f**, which by treatment with triethylamine in methanol furnished the final compounds **9a**−**f**.

Compounds **9a**−**f** were initially evaluated for their Aurora-A inhibitory activity in a biochemical assay and their ability to block cell proliferation (Table 2). Accumulation of cells with ≥4 N DNA content, the phenotype typically induced by most known Aurora inhibitors is an indication for inhibiting also Aurora-B.[13,14]

Data shown in Table 2 indicate that the benzylic substitution at the pro-R position significantly increases inhibitory potency in this series and resulted in compounds endowed with potent antiproliferative and cell cycle block activity.

To confirm the binding hypothesis, the structure of Aurora-A was solved in complex with compound **9d**. Although the crystals only diffracted to 3 Å, the electron density for the inhibitor clearly showed that the compound bound as expected, with the benzyl group positioned as the thiophene of the previous structure and the amino nitrogen of Lys 162 within hydrogen-bonding distance of the oxygen of the pro-R methoxy substituent (2.6 Å; see Supporting Information). In contrast, when data were collected from crystals of Aurora-A in complex with a compound with a methyl group at the pro-S position (**9e**), the

Scheme 1

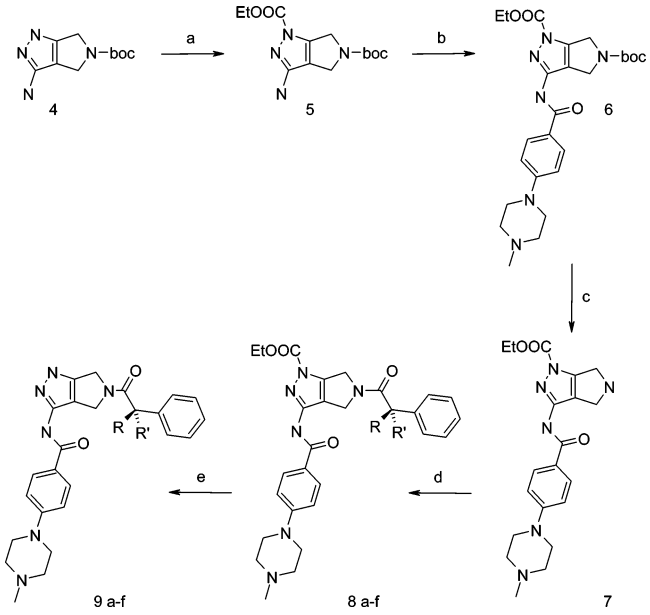

Reactants and conditions: (a) EtCOOCl, THF, 20 h, 22 °C; (b) p-piperazinylbenzoic acyl chloride, DIEA, THF, 16 h, 22 °C; (c) HCl (12 equiv, 4 N in dioxane), DCM, 24 h, 22 °C; (d) acylchloride, DIEA, DCM 6−8 h, 22 °C, or carboxylic acid, TBTU, DIEA, DMF, 24 h, 22 °C; (e) Et_3N 10% in MeOH, 3−6 h, 22 °C.

Table 2. Structure and Aurora-A Inhibition of 5-α-Substituted-(phenylacetyl)pyrrolopyrazoles

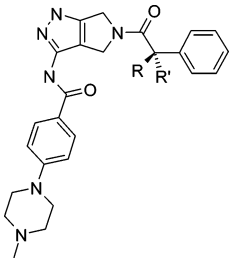

			Aur−A	Aur−B	HCT−116	
cmpd	R	R′	inhibition IC_{50},[a] nM	inhibition IC_{50},[a] nM	anti-proliferation IC_{50},[a] nM	cell cycle block EC_{50},[a,b] nM
2	H	H	130	n.t.	220	500
9a	F	H	9	300	50	110
9b	OH	H	6	48	97	>200[c]
9c	Me	H	24	99	21	100
9d	OMe	H	13	79	31	80
9e	H	Me	452	1210	n.t.	n.t.
9f	H	OMe	354	630	n.t.	n.t.

[a] IC_{50} values are reported as the mean of at least three individual determinations. Variability around the mean was <25%. [b] Concentration to induce 50% accumulation of cells with ≥4 N DNA (G2/M and polyploidy cell populations). [c] EC_{50} comprised between 200 and 1000 nM.

associated electron density indicated that the methyl group occupied the position of the phenyl ring in **9d** and the ring position of the methoxy (unpublished). It should be noted, however, that even compound **9c**, which is unable to form a hydrogen bond with Lys 126, is much more active than the unsubstituted compound **2**.

Here we report the preliminary in vitro and in vivo profile of **9d**, which emerged from a deeper characterization of this series as the compound with the best balance in terms of tumor target kinase inhibition profile, pharmaceutical properties for development, and efficacy in animal models.

Table 3. Selectivity Profile of Compound **9d**

kinase	IC_{50},[a] μ**M**	kinase	IC_{50},[a,b] μ**M**
Aurora-A	0.013	VEGFR3	0.161
Aurora-B	0.079	C-KIT	0.407
Aurora-C	0.061	VEGFR2	0.432
ABL	0.025	CDK2/cyA	0.462
TRKA	0.030	STLK2	0.621
RET	0.031	FLT3	0.669
FGFR1	0.047	PLK1	3.5
LCK	0.155	others[c]	>10

[a] Values are the mean from two independent dose−response curves; variation was generally ±25%. [b] Kinase assays were carried out as described in ref 19. [c] LYN, IR, GSK3β, NIM-1, PAK4, p38α, PDK1, CK2, CHK1, Cdc7/Dbf4, ZAP70, PKAα, IKK2, MET, EGFR, ERK2, AKT1, IKKi, PKCβ, and SULU.

Table 4. Antiproliferative Activity of Compound **9d**

cell line	IC_{50},[a] μ**M**
HeLa	0.140
MCF7	0.080
HCT-116	0.031
A-2780	0.028

[a] Values are the mean from three or more independent dose−response curves; variation was generally 25%.

Compound **9d** was seen to be a potent, ATP-competitive inhibitor of Aurora-A kinase, with an apparent K_i value of 2.5 ± 0.3 nM. Its selectivity was evaluated in an in-house panel representing diverse families of Tyr and Ser−Thr kinases. Data reported in Table 3 show that, besides inhibiting all three Aurora kinases, **9d** also inhibits an additional set of protein kinases, namely, ABL, RET, TRKA, and FGFR1 in the nanomolar range. Notably, all of them have been independently suggested as viable targets for oncology drug discovery. In particular, the therapeutic value of Imatinib clearly validated the approach of ABL inhibition for the treatment of chronic myelogenous leukemia[15] (CML), while oncogenic activation of RET tyrosine kinase has been associated with medullary thyroid carcinomas and, together with TRKA activation, to papillary thyroid carcinomas.[16,17] In addition, the activated TRKA oncogene has been associated with other human malignancies, in particular, prostate cancer.[18]

We expect that the particular kinase inhibition profile of **9d**, in which an antimitotic activity is complemented by the inhibition of targets relevant for specific cancer types, could offer promising opportunities for clinical development and therapeutic use, although we may face the risk of a decreased tolerance in patients.

In this regard, specific studies are currently ongoing to address two crucial questions: first, whether the inhibition of these additional targets contributes to the antitumoral effects or is rather obscured by the dominant phenotype induced by aurora inhibition; and second, whether the PK/PD requirements for the inhibition in vivo of these different targets are compatible with administration schedules, which might be limited by the antimitotic nature of the compound.

Compound **9d** demonstrated potent antiproliferative activity (IC_{50} values ranging from 28 to 140 nM, Table 4) in cell lines originating from various human tumor types such as HCT-116 (colon carcinoma), A2780 (ovarian carcinoma), MCF7 (breast carcinoma), and HeLa (cervical adenocarcinoma).

Similarly to what has been described for other Aurora-A and -B inhibitors, the incubation of different tumor cell lines with **9d** results in a substantial increase in 4 N DNA and polyploid (≥8 N DNA) populations. We observed that the extent of polyploidy induction depends on the genetic background of the tested cell line (data not shown). As an example, the cell cycle profile of HCT-116 cells treated for 24 h with different concentrations of the compound is reported in Figure 2.

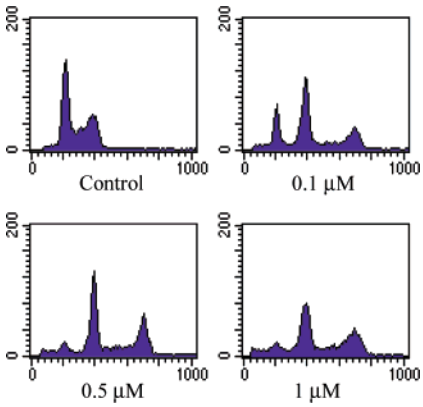

Figure 2. Flow cytometric analysis of DNA content in human colon carcinoma cells (HCT-116) treated for 24 h with increasing concentrations of **9d**.

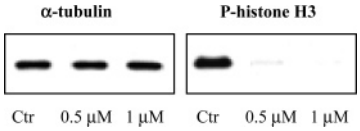

Figure 3. Western blot analysis of phospho-histone H3 in HCT-116 cells. An antibody recognizing α-tubulin was used as loading control.

Table 5. Individual and Average Pharmacokinetic Parameters Estimated in Male CD-1 Mice Following a Single IV Bolus at the Nominal Dose of 10 mg/kg with **9d** in Mice

parameter	M1	M2	M3	mean	SD
C_{max} (μ**M**)	8.0	11.1	9.6	9.6	1.5
T1/2,z (h)	0.97	1.8	1.5	1.4	0.4
AUC (μ**M·h**)	5.4	8.3	5.8	6.5	1.5
CL (L/h/kg)	4.1	2.7	4.0	3.6	0.8
V_{ss} (L/kg)	3.2	4.1	3.8	3.7	0.4

Finally, **9d** induces a complete suppression of phosphorylation of the substrate of Aurora kinases, histone H3 at serine 10, which is widely regarded as a marker of Aurora B inhibition (Figure 3).[20]

Major pharmacokinetic parameters were obtained in vivo after iv administration of 10 mg/kg of **9d** to male CD-1 mice cannulated into the superior vena cava (Table 5).

Plasma levels were detectable up to 6 h post-dosing, giving an apparent average terminal half-life of about 1.4 h. The clearance was about 70% of the hepatic blood flow and the volume of distribution higher than the total body water, indicating extensive tissue distribution.

These pharmacokinetic properties, coupled with a high aqueous solubility (>15 mg/mL as the hydrochloride salt at pH 5.5) and a high stability of the resulting solution (shelf life: 36 months at 5 °C) makes compound **9d** well-suited for development as an injectable therapeutic agent.

In vivo, **9d** was seen to be efficacious in a range of tumor models. As an example, Figure 4 illustrates the dose-dependent growth inhibition induced in the HL-60 xenograft model. Tested at doses between 7.5 mg/kg and 30 mg/kg given iv bid for 5 days, the compound showed good dose dependency and a tumor growth inhibition of up to 98%. At the highest dose (30 mg/Kg) there was evidence of tumor regression and, in two cases out of eight, cures. The maximal and reversible body weight loss at this dose was 16%.

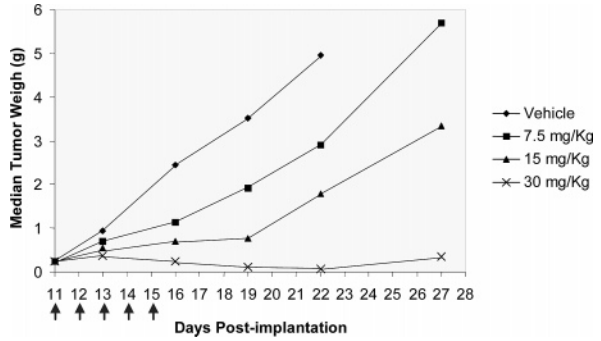

Figure 4. Antitumor activity of **9d** against HL-60 human tumor xenograft implanted in SCID mice. Arrows indicate dosing (bid × 5).

Conclusions

The data presented in this report were the starting point for a deeper evaluation of safety and efficacy of compound **9d**, which has been ultimately selected for clinical studies. The therapeutic value of compound **9d** for the treatment of both solid tumors and leukemias is currently under investigation in advanced clinical trials.

Experimental Section

All reagents and solvents were purchased from commercial suppliers of the best grade and used without further purification. Flash chromatography was performed on silica gel (Merck grade 9385, 60Å). The following chromatographic methods were used to assess compound purity. **Chromatographic Method A:** HPLC/MS was performed on a Waters X Terra RP 18 (4.6 × 50 mm, 3.5 ∝m) column using a Waters 2790 HPLC system equipped with a 996 Waters PDA detector and a Micromass mod. ZQ single quadrupole mass spectrometer, equipped with an electrospray (ESI) ion source. Mobile phase A was ammonium acetate 5 mM buffer (pH 5.5 with acetic acid/acetonitrile 95:5), and mobile phase B was H_2O/acetonitrile (5:95), with a gradient from 10 to 90% B in 8 min and hold at 90% B for 2 min. UV detection was at 220 and 254 nm. Flow rate was 1 mL/min, with an injection volume of 10 μL. A full scan was done, with a mass range from 100 to 800 amu. The capillary voltage was 2.5 KV, the source temperature was 120 °C, and the cone was 10 V. Retention times and purity refer to UV detection at 220 nm. Mass are given as the *m*/*z* ratio. **Chromatographic Method B:** HPLC was performed on a Waters X Terra RP 18 (4.6 × 50 mm, 3.5 ∝m) column using a Waters 2795 HPLC system equipped with a 996 Waters PDA detector and a S.E.D-.E.R.E Sedex 55 evaporative light scattering (ELS) detector. Mobile phase A was pH 10, 0.05% aqueous ammonia/acetonitrile (95:5), and mobile phase B was H_2O/acetonitrile (5:95), with a gradient from 10 to 90% B in 8 min and hold at 90% B for 2 min. UV detection was at 220 and 254 nm. The ELS detector conditions were as follows: gas was air, temperature was 34 °C, pressure was 2.3 bar, gain was 9, flow rate was 1 mL/min, and injection volume was 10 μL. Retention times and purity refer to ELS detection. When necessary, compounds have been purified by preparative HPLC on a Waters X-Terra RP18 (19 × 100 mm, 5 um) column using a Waters preparative HPLC2525 equipped with a 996 Waters PDA detector and a Micromass mod. ZQ single quadrupole mass spectrometer with electrospray ionization, positive mode. Mobile phase A was water with 0.01% formic acid, and mobile phase B was acetonitrile, with a gradient from 10 to 90% B in 8 min and hold 90% B for 2 min. The flow rate was 20 mL/m. ^{1}H NMR spectra were recorded on a Varian Inova 400 operating at 400.45 MHz or on a Varian Inova 500 operating at 499.76 MHz; both instruments are equipped with an Indirect Detection probe (^{1}H-{^{15}N−^{31}P}. The residual signal of the deuterated solvent was used.

Synthesis of 8a and 8c−f. The acyl chlorides, when not commercially available, were prepared according to standard procedures: oxalyl chloride (728 μL, 8.3 mmol) was added to a solution of the required acid (0.83 mmol) in DCM (10 mL) and DMF (50 μL). After stirring the mixture at room temperature overnight, volatiles were carefully removed under reduced pressure. The resulting acyl chlorides were dissolved in dichloromethane (5 mL) and added to a solution of ethyl 3-{[4-(4-methylpiperazin-1-yl)benzoyl]amino}-5,6-dihydropyrrolo[3,4-*c*]pyrazole-1(4*H*)-carboxylate trihydrochloride **7** (300 mg, 0.59 mmol) in DCM (10 mL) and DIEA (610 μL, 3.6 mmol) under stirring at room temperature. The resulting suspension was stirred 16 h at room temperature. After solvent removal, the residue was taken up with AcOEt (100 mL) and the organic layer washed with aqueous $NaHCO_3$ and brine and dried over Na_2SO_4. Solvent was evaporated, and the residue was purified on silica gel flash chromatography (DCM/MeOH, 95:5−93:7).

Synthesis of 8b. Mandelic acid (304 mg, 2 mmol) was dissolved in DMF (10 mL), DIPEA (650 mg, 5 mmol), and TBTU (740 mg, 2.4 mmol) were added, and the mixture was stirred for 15 min at room temperature.

3-{[4-(4-Methylpiperazin-1-yl)benzoyl]amino}-5,6-dihydropyrrolo[3,4-*c*]pyrazole-1(4*H*)-carboxylate trihydrochloride **7** (508 mg, 1 mmol) was added in one portion, and the mixture was stirred 8 h at room temperature. DCM (50 mL) was added, and the organic layer was washed with water and saturated aqueous $NaHCO_3$ and dried over Na_2SO_4, and the solvent was evaporated. The crude residue was purified by silica gel flash chromatography (DCM/MeOH, 80:20) to give 160 mg of the title compound (25%).

Synthesis of 9a−f. A solution of **8a−f** (0.19mmol) in MeOH (5 mL) and Et_3N (0.32 mL) was stirred at 30 °C for 3 h. The resulting mixture was evaporated under reduced pressure, and the residue was taken up with Et_2O and re-evaporated (three times). The final compounds were purified by crystallization (MeOH/H_2O; **9b**), silica gel flash chromatography (DCM/MeOH, 9:1; **9a** and **9c−e**), and preparative HPLC (**9f**).

Acknowledgment. The authors are grateful to the group of Biochemical Screening of Nerviano Medical Science; in particular, Dr. Cristina Alli has been precious with her contribution to the selectivity profile of our best compounds.

Note Added after ASAP Publication. The Conclusions paragraph was omitted and a typographical change was made in the Introduction section in the version published ASAP November 1, 2006; the corrected version was published ASAP November 6, 2006.

Supporting Information Available: Atomic coordinates and experimental structure factors have been deposited in the PDB. The complex with compound **3** has been given code 2j4z and that with **9c** has been given code 2j50. Analytical characterization of compounds **9a−f**, crystallographic methods, Aurora assay, cell proliferation assay, cell cycle analysis by flow cytometry, and Western blot analysis. This material is available free of charge via the Internet at http://pubs.acs.org.

References

(1) Matthews, N.; Visintin, C.; Hartzoulakis, B.; Jarvis, A.; Selwood, D. L. Aurora A and B kinases as targets for cancer: will they be selective for tumors? *Expert Rev. Anticancer Ther.* **2006**, *6* (1), 109−120.
(2) Marumoto, T.; Zhang, D.; Saya, H. Aurora-A—a guardian of poles. *Nat. Rev. Cancer* **2005**, *5* (1), 42−50.
(3) Bischoff, J. R.; Anderson, L.; Zhu, Y.; Mossie, K.; Ng, L.; Souza, B.; Schryver, B.; Flanagan, P.; Clairvoyant, F.; Ginther, C.; Chan, C. S.; Novotny, M.; Slamon, D. J.; Plowman, G. D. A homolog of Drosophila aurora kinase is oncogenic and amplified in human colorectal cancers. *EMBO J.* **1998**, *17* (11), 3052−3065.
(4) Warner, S. L.; Bearss, D. J.; Han, H.; Von Hoff, D. D. Targeting Aurora-2 kinase in cancer. *Mol. Cancer Ther.* **2003**, *2* (6), 589−95.
(5) Bar-Shira, A.; Pinthus, J. H.; Rozovsky, U.; Goldstein, M.; Sellers, W. R.; Yaron, Y.; Eshhar, Z.; Orr-Urtreger, A. Multiple genes in human 20q13 chromosomal region are involved in an advanced prostate cancer xenograft. *Cancer Res.* **2002**, *62*, 6803−6807.

(6) Bischoff, J. R.; Anderson, L.; Zhu, Y.; Mossie, K.; Ng, L.; Souza, B.; Schryver, B.; Flanagam, P.; Clairvoyant, F.; Ginther, C.; Chan, C. S.; Novotny, M.; Slamon, D. J.; Plowman, G. D. A homolog of Drosophila aurora kinase is oncogenic and amplified in human colorectal cancers. *EMBO J.* **1998**, *17*, 3052−3065.
(7) Wang, X.; Zhou, Y. X.; Qiao, W.; Tominaga, Y.; Ouchi, M.; Ouchi, T.; Deng, C. X. Overexpression of aurora kinase A in mouse mammary epithelium induces genetic instability preceding mammary tumor formation. *Oncogene* **2006**, May 22; Epub ahead of print.
(8) Harrington, E. A.; Bebbington, D.; Moore, J.; Rasmussen, R. K.; Ajose-Adeogun, A. O.; Nakayama, T.; Graham, J. A.; Demur, C.; Hercend, T.; Diu-Hercend, A.; Su, M.; Golec, J. M. C.; Miller, K. M. X-680, a potent and selective small-molecule inhibitor of the Aurora kinases, suppresses tumor growth in vivo. *Nat. Med.* **2004**, *10* (3), 262−327.
(9) Manfredi, M.; Ecsedy, J.; Meetze, K.; Balani, S.; Burenkova, O.; Chen, W.; Hoar, K.; Huck, J.; Leroy, P.; Sells, T.; Stroud, S.; Vos, T.; Weatherhead, G.; Wysong, D.; Zhang, M.; Claiborne, C. MLN8054, an orally active Aurora A kinase small molecule inhibitor in phase I clinical trials. 97th Annual AACR Meeting, Washington, DC, 2006, Abstract 4724.
(10) Wilkinson, R. W.; Keen, N.; Odedra, R.; Heaton, S. P.; Wedge, S. R.; Foote, K. M.; Mortlock, A.; Jung, F.; Heron, N. M.; Brady, M. C.; Walker, M.; Khatri, L.; Barrass, N. C.; Foster, J. J.; Green, S. AZD1152: A highly potent and specific aurora kinase inhibitor. 97th Annual AACR Meeting, Washington, DC, 2006, Abstract 5673.
(11) Fancelli, D.; Berta, D.; Bindi, S.; Cameron, A.; Cappella, P.; Carpinelli, P.; Catana, C.; Forte, B.; Giordano, P.; Giorgini, M. L.; Vulpetti, A.; Mantegani, S.; Marsiglio, A.; Meroni, M.; Moll, J.; Pittalà, V.; Roletto, F.; Severino, S.; Soncini, C.; Storici, P.; Tonani, R.; Varasi, M.; Vianello, P. Potent and selective Aurora inhibitors identified by the expansion of a novel scaffold for protein kinase inhibition. *J. Med. Chem.* **2005**, *48* (8), 3080−3084.
(12) Soncini, C.; Carpinelli, P.; Gianellini, L.; Fancelli, D.; Vianello, P.; Rusconi, L.; Storici, P.; Zugnoni, P.; Pesenti, E.; Croci, W.; Ceruti, R.; Giorgini, M. L.; Cappella, P.; Ballinari, D.; Sola, F.; Varasi, M.; Bravo, R.; Moll, J. PHA-680632, a novel Aurora kinase inhibitor with potent antitumoral activity. *Clin. Cancer Res.* **2006**, *12* (13), 4080−4089.
(13) Terada, Y.; Tatsuka, M.; Suzuki, F.; Yasuda, Y.; Fujita, S.; Otsu M.; AIM-1: A mammalian midbody-associated protein required for cytokinesis. *EMBO J.* **1998**, *17*, 667−676.
(14) Ditchfield, C.; Johnson, V. L.; Tighe, A.; Ellston, R.; Haworth, C.; Johnson, T.; Mortlock, A.; Keen, N.; Taylor S. S.; Aurora B couples chromosome alignment with anaphase by targeting BubR1, Mad2, and Cenp-E to kinetochores. *J. Cell Biol.* **2003**, *161*, 267−280.
(15) Jones, R. L.; Judson, I. R. The development and application of imatinib. *Exp. Opin. Drug Safety* **2005**, *4* (2), 183−191.
(16) Kouvaraki, M. A.; Shapiro, S. E.; Perrier, N. D.; Cote, G. J.; Gagel, R. F.; Hoff, A. O.; Sherman, S. I.; Lee, J. E.; Evans, D. B. RET proto-oncogene: a review and update of genotype-phenotype correlations in hereditary medullary thyroid cancer and associated endocrine tumors. *Thyroid* **2005**, *15* (6), 531−544.
(17) Greco, A.; Mariani, C.; Miranda, C.; Lupas, A.; Pagliardini, S.; Pomati, M.; Pierotti, M. A. The DNA rearrangement that generates the TRK-T3 oncogene involves a novel gene on chromosome 3 whose product has a potential coiled-coil domain. *Mol. Cell. Biol.* **1995**, *5* (11), 6118−6127.
(18) George, D. J.; Suzuki, H.; Bova, G. S.; Isaacs, J. T. Mutational analysis of the TrkA gene in prostate cancer. *Prostate* **1998**, *36* (3), 172−180.
(19) Pevarello, P.; Brasca, G. M.; Amici, R.; Orsini, P.; Traquandi, G.; Corti, L.; Piutti, C.; Sansonna, P.; Villa, M.; Pierce, B. S.; Pulici, M.; Giordano, P.; Martina, K.; Fritzen, E. L.; Nugent, R. A.; Casale, E.; Cameron, A.; Ciomei, M.; Roletto, F.; Isacchi, A.; Fogliatto, G.; Pesenti, E.; Pastori, W.; Marsiglio, A.; Leach, K. L.; Clare, P. M.; Fiorentini, F.; Varasi, M.; Vulpetti, A.; Warpehoski, M. A. 3-Aminopyrazole inhibitors of CDK2/cyclin A as antitumor agents. 1. Lead finding. *J. Med. Chem.* **2004**, *47* (13), 3367−3380.
(20) Crosio, C.; Fimia, G. M.; Loury, R.; Kimura, M.; Okano, Y.; Zhou, H.; Sen, S.; Allis, C. D.; Sassone-Corsi, P. Mitotic phosphorylation of histone H3: spatio-temporal regulation by mammalian Aurora kinases. *Mol. Cell. Biol.* **2002**, *22* (3), 874−885.

JM060897W